

Characterization and Control of Insulated Gate Interfaces on GaN-Based Heterostructures

Tamotsu Hashizume^{1,2} and Masamichi Akazawa¹

¹Research Center for Integrated Quantum Electronics, Hokkaido University, Japan

²JST-CREST, Japan

e-mail: hashi@rciqe.hokudai.ac.jp

To improve stability and reliability of GaN FETs, it is essential to fabricate well-controlled MOS gate structures with low electronic state densities at insulator/(Al)GaN interfaces. An aluminum oxide (Al_2O_3) film is one of the best candidates for a gate insulator because it has large band gap against GaN and AlGaN, high breakdown field and high permittivity. In this paper, we report on the characterization and control of GaN-based MOS structures, focusing on the electronic states at the $\text{Al}_2\text{O}_3/\text{AlGaN}$ interfaces prepared by atomic layer deposition (ALD).

The undoped $\text{Al}_{0.26}\text{Ga}_{0.74}\text{N}/\text{undoped GaN}$ heterostructure grown on a sapphire substrate by metal organic chemical vapor deposition was used in this work, as shown in Fig. 1. The sheet resistance and mobility of the AlGaN/GaN heterostructure were $480 \text{ } \Omega/\text{sq.}$ and $1550 \text{ cm}^2/\text{Vs}$, respectively. An Al_2O_3 film with a nominal thickness of 20 nm was then deposited on the AlGaN surface using an ALD system (SUGA-SAL100H) at $250 \text{ }^\circ\text{C}$ for 170 cycles. In the ALD process, water vapor and trimethylaluminium (TMA) were introduced into an ALD reactor in alternate pulse forms. The deposition rate of Al_2O_3 was 0.11 nm/cycle .

Figure 2 shows the experimental C–V and G/w–V curves of the 20-nm- $\text{Al}_2\text{O}_3/\text{AlGaN}/\text{GaN}$ structure. In the bias range from -7 to 1V , we observed an almost constant capacitance corresponding to the series capacitance of Al_2O_3 and AlGaN layers (C_{TOTAL}). At around $V_G = -8 \text{ V}$, a steep decrease in capacitance was observed, indicating the 2DEG depletion. At a forward bias of $+1\text{V}$, a steplike increase in capacitance occurred, reflecting the electron transfer from the AlGaN/GaN to $\text{Al}_2\text{O}_3/\text{AlGaN}$ interfaces.

To understand this C–V behavior, we calculated C–V curves and corresponding band diagrams. The calculation was carried out using a numerical solver of the Poisson equation based on the one-dimensional Gummel algorithm, taking into account the fixed charge at the AlGaN/GaN interface originating from spontaneous and piezoelectric polarization as well as the charge in the electronic state at the $\text{Al}_2\text{O}_3/\text{AlGaN}$ interface [1, 2]. The interface state density distribution used in the calculation and the calculated C–V curves are shown in Figs. 3 and 4. All the calculated curves showed the two-step behavior, as observed in the experimental C–V result. At around the forward bias near step 1, the nearly flat potential of the AlGaN layer shown in Fig. 5(a) can lead to the electron transfer from the AlGaN/GaN to $\text{Al}_2\text{O}_3/\text{AlGaN}$ interfaces.

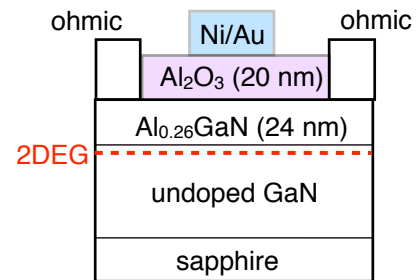


Fig. 1 $\text{Al}_2\text{O}_3/\text{AlGaN}/\text{GaN}$ structure

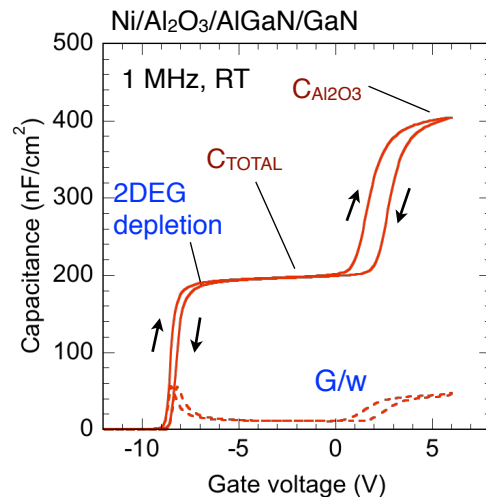


Fig. 2 Admittance characteristics of $\text{Al}_2\text{O}_3/\text{AlGaN}/\text{GaN}$ structure.

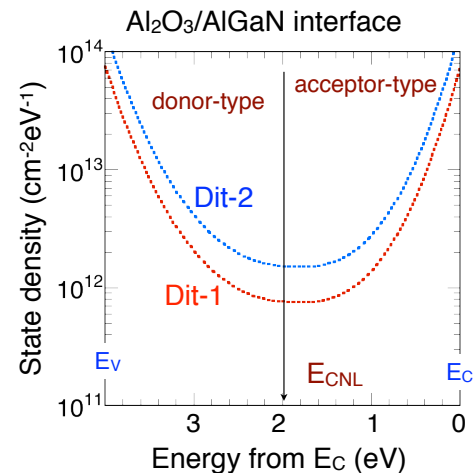


Fig. 3 Interface state density distributions used in the C–V calculation.

However, at the same time, there is a high possibility of electron trapping at the $\text{Al}_2\text{O}_3/\text{AlGaN}$ interface states. The acceptor-type states produce negative charges when they trap electrons. Such negatively charged interface states screen the gate electric field, causing the voltage shift at step 1 and the stretch out (decrease) of the C - V slope. On the other hand, the stretch-out behavior was not observed at step 2 in the experimental C - V curve (Fig. 2), which is consistent with the calculation result. Figure 5(b) shows a potential distribution at $V_G = -8$ V. In this bias region, the Fermi level is located far below the valence band maximum of AlGaN at the $\text{Al}_2\text{O}_3/\text{AlGaN}$ interface. The electron occupation of interface states is no longer a function of the gate bias. Additionally, it is estimated that the time constant of electron emission from the interface states near the midgap or deeper in energies exceeds 10^{20} s at room temperature. This leads to the fact that the interface states act as “fixed and frozen charges”, and thus the stretch out of the C - V curve was not observed at step 2. It is thus very difficult to detect interface states by a standard C - V measurement at RT.

To overcome this difficulty, we have developed a photoassisted C - V analysis utilizing photons with energies lower than the AlGaN bandgap [2]. First, as shown in Fig.6, we swept the gate voltage from +5 to -12 V under a dark condition. Then, the gate voltage was kept at -12 V and the monochromatic light with a photon energy ($h\nu$) less than the bandgap of AlGaN was illuminated to the sample surface for 120 s. Then we turned off the light and restarted the C - V measurement. Consequently, we observed the parallel C - V shift originating from the photoassisted electron emission from the interface states with the energy range corresponding to the photon energy range. When the sample surface was illuminated with a higher photon energy, a larger amount of photoassisted electron emission causes the larger V_{TH} shifts in C - V curves. The accurately parallel C - V shift toward the negative direction indicates that the interface states at $\text{Al}_2\text{O}_3/\text{AlGaN}$ act as fixed and frozen charges in this bias range. The V_{TH} difference (ΔV_2) between two photon energies corresponds to the interface charge difference. We thus simply estimated the interface state densities. It was found that the $\text{Al}_2\text{O}_3/\text{AlGaN}$ interface included interface states with densities higher than $1 \times 10^{12} \text{ cm}^{-2} \text{ eV}^{-1}$.

References

- [1] M. Miczek, C. Mizue, T. Hashizume, and B. Adamowicz, *J. Appl. Phys.* **103**, 104510 (2008).
- [2] C. Mizue, Y. Hori, M. Miczek, and T. Hashizume: *Jpn. J. Appl. Phys.* **50**, 021001(2011).

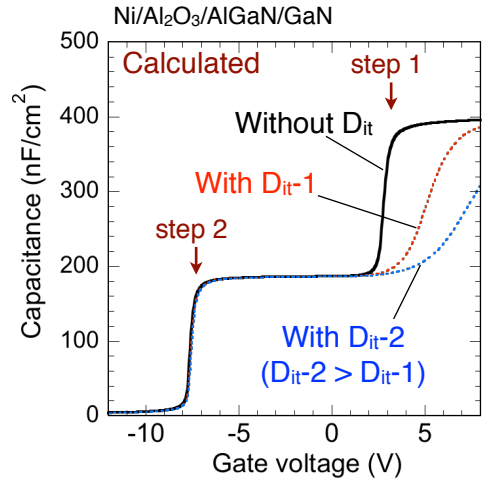


Fig. 4 Calculated C - V curves of $\text{Al}_2\text{O}_3/\text{AlGaN}/\text{GaN}$ structure.

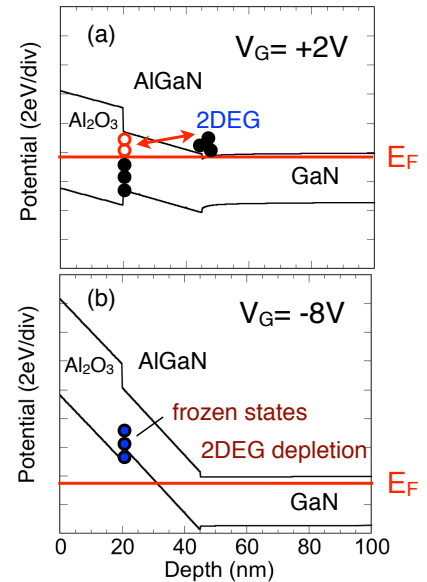


Fig. 5 Band diagram of $\text{Al}_2\text{O}_3/\text{AlGaN}/\text{GaN}$ structure.

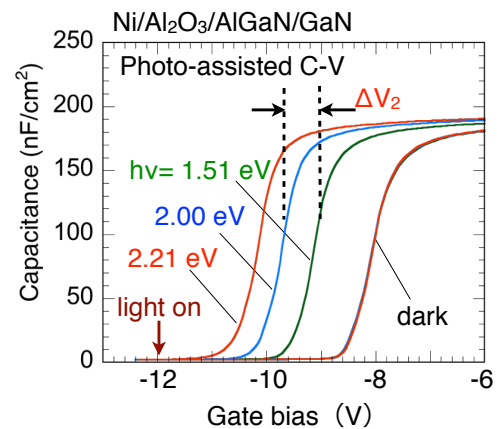


Fig. 6 Photoassisted C - V characteristics of $\text{Al}_2\text{O}_3/\text{AlGaN}/\text{GaN}$ structure.

